Chemistry–A European Journal
Research Article
doi.org/10.1002/chem.202401015
Chemistry Europe
European Chemical Societies Publishing
www.chemeurj.org

Hot Paper

Investigation of Isolated IrF_5^-, IrF_6^- Anions and $M[IrF_6]$ (M = Na, K, Rb, Cs) Ion Pairs by Matrix-Isolation Spectroscopy and Relativistic Quantum-Chemical Calculations

Yan Lu,[a] Artur Wodyński,[b] Marc Reimann,[b] Robert Medel,[a] Martin Kaupp,*[b] and Sebastian Riedel*[a]

The molecular IrF_5^-, IrF_6^- anions and $M[IrF_6]$ (M = Na, K, Rb, Cs) ion pairs were prepared by co-deposition of laser-ablated alkali metal fluorides MF with IrF_6 and isolated in solid neon or argon matrices under cryogenic conditions. The free anions were obtained as well by co-deposition of IrF_6 with laser-ablated metals (Ir or Pt) as electron sources. The products were characterized in a combined analysis of matrix IR spectroscopy and electronic structure calculations using two-component quasi-relativistic DFT methods accounting for spin-orbit coupling (SOC) effects as well as multi-reference configuration-interaction (MRCI) approaches with SOC. Inclusion of SOC is crucial in the prediction of spectra and properties of IrF_6^- and its alkali-metal ion pairs. The observed IR bands and the computations show that the IrF_6^- anion adopts an O_h structure in a nondegenerate ground state stabilized by SOC effects, and not a distorted D_{4h} structure in a triplet ground state as suggested by scalar-relativistic calculations. The corresponding "closed-shell" $M[IrF_6]$ ion pairs with C_{3v} symmetry are stabilized by coordination of an alkali metal ion to three F atoms, and their structural change in the series from M = Na to Cs was proven spectroscopically. There is no evidence for the formation of IrF_7, IrF_7^- or $M[IrF_7]$ (M = Na, K, Rb, Cs) ion pairs in our experiments.

Introduction

The electronic molecular structure of heavy group 10 hexafluorides, which exhibit $(t_{2g})^4$ non-bonding molecular orbitals, has attracted substantial interest in the past few years due to the competition between Jahn–Teller (JT) distortion and spin-orbit coupling (SOC) effects.[1–8] A JT-distorted $^3A_{1g}/D_{4h}$ structure has been predicted as the ground state for the hitherto hypothetical PdF_6 in scalar-relativistic calculations without SOC contribution.[1,7] However, when SOC is taken into account, a D_{3d} structure also becomes energetically competitive with the D_{4h} and O_h structures. It was therefore suggested that PdF_6 would be highly fluxional and most likely would exhibits an average O_h structure under most experimental conditions.[7] This would be in line with four-component relativistic Dirac–Hartree–Fock (DHF) calculations where the JT distortion of PdF_6 is quenched by SOC and a diamagnetic, octahedral singlet structure is predicted.[4] However, the exact prediction of the structure as well as the electronic configuration is still challenging, especially if there is no convincing experimental evidence for the existence of PdF_6.[1,9] For the heavier PtF_6, relativistic effects like SOC become more pronounced, and its inclusion in computations changes the ground state from a D_{4h} triplet[10] to a nondegenerate state with O_h symmetry consistent with various spectroscopic observations.[11,12] This holds at two-component X2C and four-component relativistic DHF and Dirac–DFT levels.[2,4–6,13] David *et al.* reported that the Dirac–LDA calculations afford SOC splittings of 1326.4 and 4376.4 cm^{-1} for PdF_6 and PtF_6, respectively.[4]

Based on these interesting results for the palladium and platinum hexafluorides, it is interesting to investigate the isoelectronic $5d^4$ anion IrF_6^-. This anion was predicted by scalar-relativistic coupled-cluster calculations to show a distorted triplet ground state[10] while two-component ZORA–DFT calculations suggested D_{3d} and D_{4h} structures which are very similar in energy.[10] Experimental evidence from solid-state high-resolution ^{19}F NMR data favors a nondegenerate octahedral "diamagnetic" complex IrF_6^- in $K[IrF_6]$.[8] Indeed, relativistic Dirac–DFT computations including SOC suggested an octahedral "singlet".[14] Experimental SO splittings of IrF_6^- (3400 cm^{-1}) are found to be lower than for PtF_6 (5200 cm^{-1}), in keeping with the trend of calculated λ^{so} values of $K[IrF_6]$ (10256 cm^{-1}) and PtF_6 (12082 cm^{-1}) at Dirac–Fock level.[8,11,12,15] Moreover, solid-state $[H_2F]^+[IrF_6]^-$ is EPR-silent, and $K[IrF_6]$ and $Cs[IrF_6]$ display

[a] Y. Lu, Dr. R. Medel, Prof. Dr. S. Riedel
Institut für Chemie und Biochemie-Anorganische Chemie
Freie Universität Berlin
Fabeckstrasse 34/36, 14195 Berlin, Germany
E-mail: s.riedel@fu-berlin.de

[b] Dr. A. Wodyński, Dr. M. Reimann, Prof. Dr. M. Kaupp
Institut für Chemie Theoretische Chemie/Quantenchemie
Technische Universität Berlin
Sekr. C7, Strasse des 17. Juni 135, 10623 Berlin, Germany
E-mail: martin.kaupp@tu-berlin.de

Supporting information for this article is available on the WWW under https://doi.org/10.1002/chem.202401015

temperature-independent paramagnetism. All of these data favor a nondegenerate ground state for IrF_6^-.[8,16,17]

To the best of our knowledge, the free IrF_6^- anion has not yet been experimentally detected and known experimental data are all based on solid salts.[8,15,16,18,19–21] Although its alkali metal salts M[IrF_6] have been characterized by single-crystal[20–22] and synchrotron X-ray powder diffraction (SPDD),[19] there is a lack of experimental spectroscopic or theoretical investigations on the molecular M[IrF_6] (M = Na, K, Rb, Cs) ion pairs. Additionally, the lower-valent pentafluoroiridate(IV) anion IrF_5^- has not yet been studied spectroscopically, nor is its solid-state structure known in salts, in contrast to many investigations on iridium(IV) complexes containing $[IrF_6]^{2-}$ units involving various counterions.[20,23] Finally, the high-valent anion IrF_7^- was only investigated computationally,[10] while the possible existence of $[NO]^+[IrF_7]^-$ as a reaction intermediate has been postulated.[24] A recent study reported an unsuccessful attempt for the preparation of Cs[IrF_7] salt.[21]

The combination of laser ablation and matrix-isolation spectroscopy has proven to be a powerful method for producing novel unstable anionic species.[25–29] In our previous reports, non-metal F_3^- and F_5^- anions were formed after condensation of F_2 with laser-ablated metal atoms as electron sources.[25,26,30] Therefore, the molecular IrF_6^- anion might be expected to be formed by electron capture by neutral IrF_6 molecules during the laser ablation process. Additionally, the successful preparation and identification of the alkali metal ion pairs M[F_3][25,26,31] and M[AuF_4][32] formed by the reaction of MF with F_2, and MF with AuF_3, respectively, in solid noble gases may suggest the possible identification of molecular M[IrF_7] (M = Na, K, Rb, Cs) ion pairs via the laser ablation of the corresponding alkali metal fluorides MF with IrF_6.

Herein, we report for the first time on the preparation and matrix-isolation IR spectroscopic characterization as well as accompanying relativistic quantum-chemical studies of the electronic structures of molecular IrF_5^-, IrF_6^- anions and M[IrF_6] (M = Na, K, Rb, Cs) alkali ion pairs. These products were generated by the laser ablation of alkali metal fluorides MF with IrF_6 in cryogenic solid neon or argon matrices. Both of the free anions were also detected in separate matrix-isolation experiments based on laser ablation of metals (Ir or Pt) as electron sources in the presence of IrF_6. Their identification is based on the experimental Ir–F stretching vibrational frequencies and further supported by two-component quasi-relativistic DFT computations[33] as well as MRCI computations[34–36] including SOC effects. Electron affinities and fluoride ion affinities of IrF_6 and IrF_5 have also been calculated.

Results and Discussion

Computational Results

The structures of IrF_5^-, IrF_6^- and the M[IrF_6] (M = Na, K, Rb, Cs) ion pairs in their ground states were optimized using two-component (2c-X2C) all-electron density functional theory (DFT) calculations, as depicted in Figure 1. These optimizations utilized 1c-X2C calculations with selected multiplicities as starting points (optimized 1c-X2C structures are presented in Figures S1 and S2 in Supporting Information). Optimization at 2c-X2C level was performed in C_1 symmetry, allowing for slight deviations from the initial higher-symmetric structures. We note that after incorporation of the substantial SOC in the 2c calculations, spin is not a good quantum number anymore. When discussing spin multiplicities for the 2c calculations, we refer exclusively to the multiplicity of the Kohn-Sham orbital guess employed. We denote the electronic configuration states as pseudo multiplicities, indicating that these refer solely to the 1c configurations used as initial guesses.

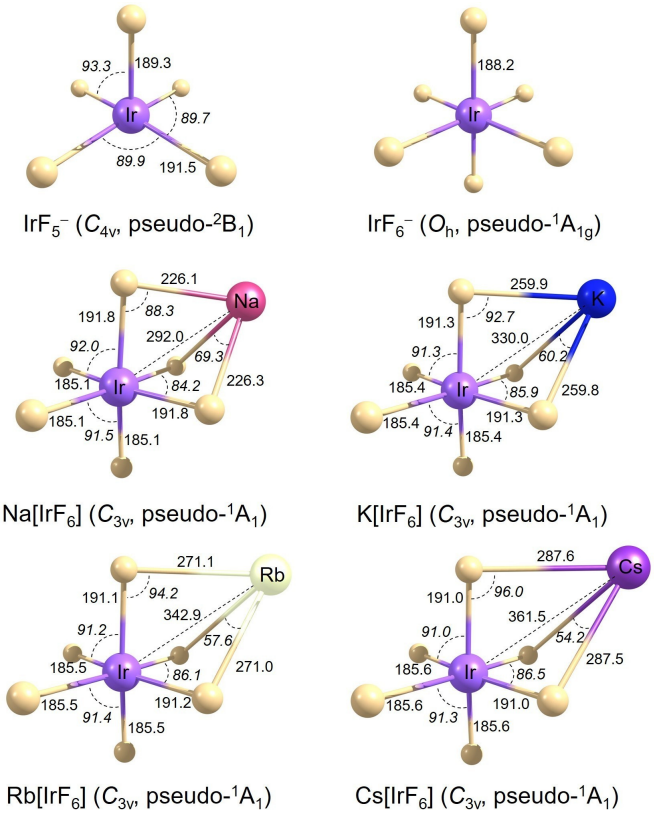

Figure 1. Molecular structures of M[IrF_6] (M = Na, K, Rb, Cs) ion pairs and IrF_5^- and IrF_6^- anions in their ground states obtained at the 2c-X2C-PBE0-D3(BJ)/x2c-TZVPall-2c (M[IrF_6]) and 2c-X2C-PBE0/x2c-TZVPall-2c (anions) levels. Selected bond lengths (pm) and angles (°, in *italics*) are shown. Optimization at 2c-X2C level was performed in C_1 symmetry.

The IrF_5^- anion, in its pseudo-doublet ground state, shows a C_{4v}-symmetric (square-pyramidal) structure characterized by an axial and four longer equatorial Ir–F bonds. This agrees with previous predictions for the IrF_5 and PtF_5 molecules.[5,37] Due to numerical reasons, our DFT-optimized structures show slight distortions from perfect C_{4v}. For the IrF_6^- anion, 2c-X2C DFT calculations incorporating SOC revealed that, in contrast to scalar-relativistic predictions indicating a $^3A_{1g}/D_{4h}$ ground state (as shown in Figure S1), the ground state is a Kramers-restricted pseudo-closed-shell one with O_h symmetry. The pseudo-triplet configuration was found to be energetically less favourable, lying 22–27 kJ/mol above the ground state. It is worth mentioning that 2c-X2C calculations may converge to two

distinct pseudo-open-shell electronic configurations depending on the initial 1c-X2C guess used. One of these configurations, despite being slightly lower in energy than the Kramers–restricted pseudo-closed-shell configuration, was identified as exhibiting broken symmetry and is thus excluded from further analysis (detailed information can be found in Comment S1 in Supporting Information). We observed similar behavior for the isoelectronic PtF_6.[5]

We note that the octahedral symmetry of the ground state of IrF_6^- (or of PdF_6 and PtF_6) can be justified without the use of explicit spin-multiplicities: in an O_h-symmetric configuration, IrF_6^- exhibits (in the non-relativistic limit) a $^3T_{1g}$ ground state (see Figure 2). As this is an orbital-degenerate state, it will experience Jahn-Teller (JT) distortion towards D_{4h} symmetry in such a manner that the ground state becomes nondegenerate. This $^3A_{2g}$ state, however, is still triply degenerate in the spin-domain, leading to, for example, an EPR signal. Under strong spin-orbit coupling (SOC), the $^3T_{1g}$ state splits into several different states upon coupling of the orbital and the spin functions,[38] leading to four states, $T_{1g}\otimes T_{1g} = A_{1g}\otimes E_g\otimes T_{1g}\otimes T_{2g}$, for which spin is no longer a good quantum number. Using configurational energies obtained at the 1c-X2C-MRCI+Q level (see Computational Details) to diagonalize the SOC matrix, we arrive at the diagram shown on the right-hand site of Figure 2. The ground state is totally symmetric and will therefore not exhibit JT distortion. We also do not expect an EPR signal or temperature-dependent paramagnetism, as the first excited T_{1g} state is too high in energy (ca. 4500 cm^{-1}) to be accessible thermally or via typical microwave frequencies used for EPR. This result can be directly transferred to PdF_6 and PtF_6 and potentially other d^4 systems with strong spin-orbit coupling. It provides a more precise description of the electronic states of IrF_6^- than the 2c-DFT calculations shown above.

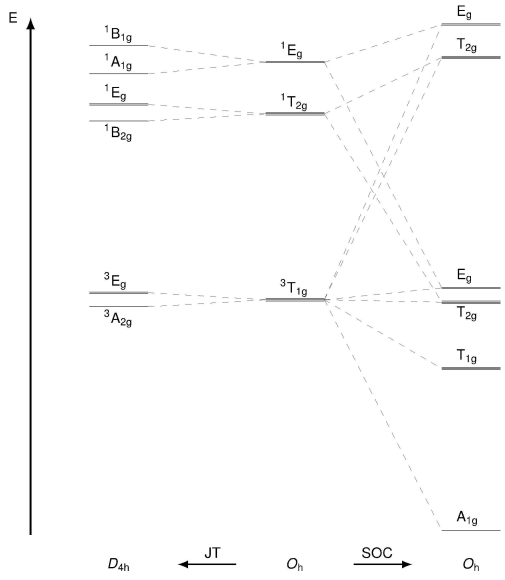

Figure 2. Semi-quantitative state diagram of IrF_6^- in the scalar-relativistic limit and perfect O_h symmetry (middle) and under JT distortion to D_{4h} (left) or when considering SOC (right). State energies were calculated at the MRCI+Q level (see Computational Details) using symmetrized structures obtained at the 2c-X2C-PBE0 level.

2c-X2C DFT structure optimizations of $M[IrF_6]$ ion pairs (M = Na, K, Rb, Cs) provide C_{3v}-symmetrical structures, characterized by an alkali metal atom being coordinated by three fluorine atoms from the IrF_6 moiety, as illustrated in Figure 1. The optimizations were performed for the Kramers-restricted pseudo-closed-shell ground state to be consistent with the results obtained for the isolated anion (see above).

Experimental Results

Laser Ablation of Metals with IrF_6

The infrared spectra recorded after co-deposition of laser-ablated metal atoms (Ir or Pt) with IrF_6 in excess neon or argon at 5 K are shown in Figures 3 and 4. The binary fluoride molecules IrF_5 and IrF_6 as common products were observed after sample deposition. Clearly, IrF_5 is present in the matrix as a result of the homolytic cleavage of one Ir–F bond in IrF_6 by the UV radiation accompanying the laser ablation of metals.[37] Apart from the known species IrF_6 and IrF_5, new IR absorptions at 647.2/643.2 and 599.8 cm^{-1} appeared simultaneously in the neon spectra from the laser-ablation experiments using different metal (Ir or Pt) targets in the presence of IrF_6 (Figures 3(A) and 3(B)). In order to distinguish the newly formed metal-independent IR bands, further annealing and irradiation of the sample was performed (Figures 4, S5 and S6). Both absorptions in the separate Ir and Pt experiments decreased during annealing of the sample to 9 K. However, further irradiation with red light (λ = 656 nm, 20 min) increased the more intense band at 643.2 cm^{-1}, while the weaker band at 599.8 cm^{-1} decreased slightly, indicating that two new species were formed in neon matrices. Analogous spectra from separate Ir and Pt experiments were also recorded after sample deposition in solid argon (Figures 3(C) and 3(D)). However, in this case only one

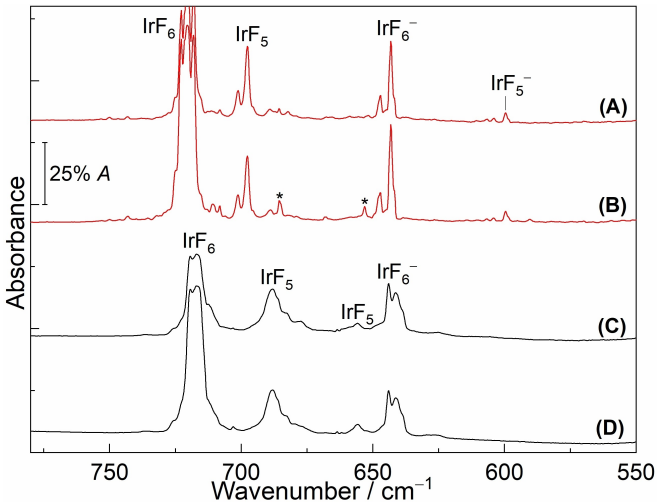

Figure 3. Infrared matrix-isolation spectra of neon (**A** and **B**) and argon (**C** and **D**) matrices at 5 K. (**A**) and (**C**) are spectra of the reaction products from laser ablation of Pt with IrF_6. (**B**) and (**D**) are spectra of the reaction products from laser ablation of Ir with IrF_6. The bands marked with asterisks were not assigned.

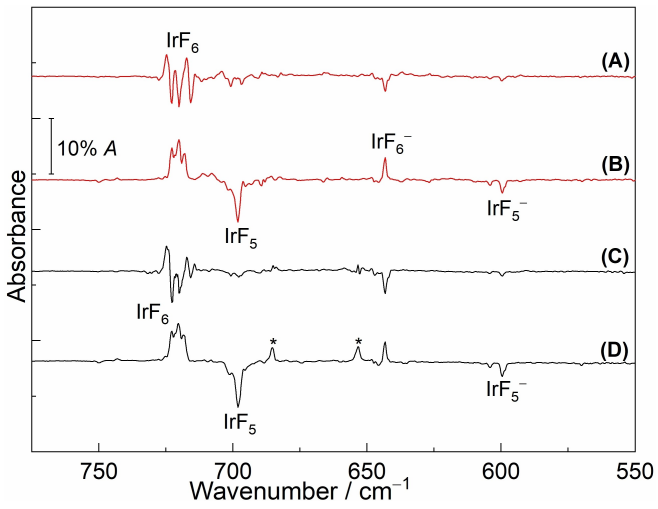

Figure 4. Infrared matrix-isolation spectra of neon matrices at 5 K. (**A**) IR difference spectrum reflecting the changes of the reaction products from laser ablation of Pt with IrF_6 upon annealing to 9 K; (**B**) IR difference spectrum reflecting the changes of the reaction products upon subsequent 656 nm LED irradiation for 20 min; (**C**) IR difference spectrum reflecting the changes of the reaction products from laser ablation of Ir with IrF_6 upon annealing to 9 K; (**D**) IR difference spectrum reflecting the changes of the reaction products upon subsequent 656 nm LED irradiation for 20 min. The bands marked with asterisks were not assigned.

Table 1. Calculated and experimentally observed IR vibrational frequencies (in cm^{-1}) of the IrF_5^- and IrF_6^- anions.[a]

Species	Sym.	Calc. (Int.)[b]		Exp.	
		2c-X2C DFT		Ne	Ar
		B3LYP	PBE0		
IrF_5^- (C_{4v}, pseudo-$^2B_1$)	a_1	619.2 (6)	644.8 (8)	–[c]	–[c]
	e	585.3 (239)×2	603.7 (251)×2	599.8	–[c]
	a_1	560.9 (47)	589.1 (46)	–[c]	–[c]
	b_2	544.6 (0)	565.0 (1)	–[c]	–[c]
IrF_6^- (O_h, pseudo-$^1A_{1g}$)	T_{1u}	631.3 (219)×3	652.4 (231)×3	647.2/ 643.2	644.1/ 641.1

[a] The complete set of calculated frequencies is provided in Supporting Information (Tables S1 and S6). Intensities are shown in parentheses in km mol^{-1}. [b] x2c-TZVPall-2c basis set. [c] Bands not observed, or too weak.

new metal-independent broad band at 644.4/641.1 cm^{-1} appeared in addition to the identified IrF_6 and IrF_5 absorptions.[37]

Based on the observed metal-independent absorptions with similar photochemical and annealing behaviors in neon matrices in the Ir and Pt experiments, most likely, the two new products are IrF_6^- and IrF_5^- anions, which could be formed via electron capture by the precursor IrF_6 and the photodissociation product IrF_5. The weak metal-independent band at 599.8 cm^{-1} observed in the neon spectra is attributed to a strong equatorial asymmetric IrF_4 stretching mode of the hitherto unknown molecular IrF_5^- anion. It shows a large red-shift of 98.0 cm^{-1}, relative to the same stretching vibration in neutral IrF_5 located at 697.8 cm^{-1} in neon matrix.[37] The observed band agrees well with the predicted most intense absorption, but the computed much weaker IR-active absorption for axial Ir–F vibrational stretching of the IrF_5^- anion was not detected in our experiments (Table 1). Unfortunately, no counterpart of the 599.8 cm^{-1} band was detected in the argon matrix, which is most likely due to its low abundance.

The strong metal-independent absorptions at 643.2 cm^{-1} in neon and 641.1 cm^{-1} in argon matrices were assigned to the free IrF_6^- anion. Similar to the cases of IrF_6 (720.6 cm^{-1} in neon matrix; 719.3 cm^{-1} in argon matrix)[37] and PtF_6 (705.6 cm^{-1} in neon matrix; 705.5 cm^{-1} in argon matrix),[5] the band of IrF_6^- also shows a small matrix shift (2.1 cm^{-1}) going from argon to neon. Moreover, such a matrix shift was also observed in the AuF_4^- anion (611.3 cm^{-1} in neon matrix; 610.6 cm^{-1} in argon matrix).[39] Similar to our own 1c-X2C calculations (Table S5), previous scalar-relativistic calculations of IrF_6^- in a triplet ground state predicted a D_{4h} structure with two vibrational Ir–F bands at 650 and 615 cm^{-1} having an intensity distribution of about 1:2.[10] This clearly does not match the observed absorptions. As discussed above, our 2c-X2C calculations including SOC afford a diamagnetic octahedral structure in a Kramers-restricted pseudo-closed-shell ground state for IrF_6^-, supported by high-level MRCI+Q energy calculations with SOC. This is consistent with the single observed IR band (Table 1), the absence of an EPR signal for $[H_2F]^+[IrF_6]^-$, and the temperature-independent paramagnetism for M[IrF_6] (M=K and Cs).[8,16,17]

Laser Ablation of Alkali Metal Fluorides with IrF_6

IR spectra were recorded after co-deposition of laser-ablated alkali metal fluorides MF (M=Na, K, Rb, Cs) with IrF_6 in excess neon or argon at 5 K (Figures 5 and 6). The common absorptions assigned to the IrF_6^- and IrF_5^- anions as electron capture products (see above) were also observed in the experiments when the alkali metal fluorides were used, which further confirms the assignment of these anions. In addition to the identified species, the present experiments also led to the formation of some new bands which were found to be alkali-metal dependent and were not observed in the experiment using laser-ablated Ir with IrF_6 (Figures 5(E) and 6(E)). These bands can be grouped and belong to different vibrational modes of the same new molecule upon subsequent irradiation with light of a wavelength λ=656 nm (Figures S7–S10).

The wavenumber of the most intense Ir–F stretching band depending on the alkali metal ion of 661.9, 658.4, 657.4, and 656.7 cm^{-1} for NaF through CsF in neon matrix (656.5, 654.1, 653.0, and 652.1 cm^{-1} in argon matrix) are higher than for the isolated IrF_6^- anion at 643.2 cm^{-1} in neon and 641.2 cm^{-1} in argon matrices. This is the typical relationship for ion pairs, similar to the cases of the free AuF_4^- anion (611.3 cm^{-1} in a neon matrix)[39] and its M[AuF_4] (M=K, Rb, Cs) ion pairs (ca.

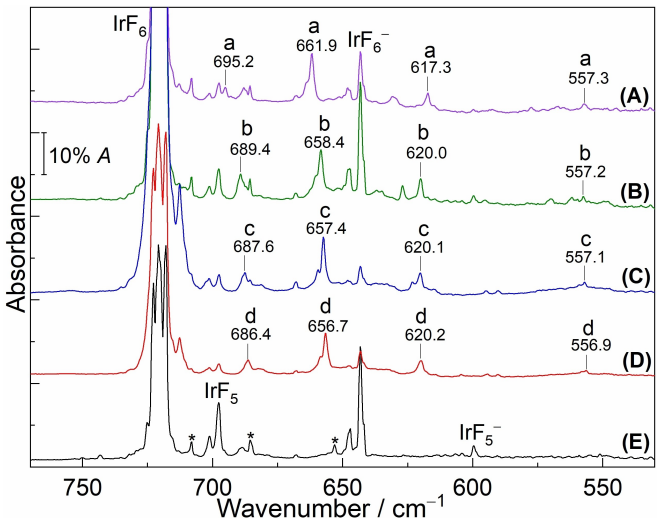

Figure 5. Infrared matrix-isolation spectra of neon matrices at 5 K. (**A**–**D**) Spectra of reaction products of laser-ablated MF (M = Na, K, Rb, Cs) with IrF_6. (**A**) NaF, (**B**) KF, (**C**) RbF and (**D**) CsF. (**E**) Spectrum of the reaction products from laser ablation of Ir with IrF_6. The IR bands of Na[IrF_6], K[IrF_6], Rb[IrF_6], Cs[IrF_6] were labeled with **a**, **b**, **c**, and **d**, respectively. The bands marked with asterisks were not assigned.

632 cm^{-1} in a neon matrix).[32] Therefore, the IrF_6^- anion trapped in solid neon or argon is most likely coordinated by an alkali metal atom, and the observed alkali-metal dependent bands can be assigned to the M[IrF_6] (M = Na, K, Rb, Cs) ion pairs. Unfortunately, the highest-frequency Ir–F stretching band in the series of the M[IrF_6] ion pairs located at 695.2, 689.4, 687.6, and 686.4 cm^{-1}, respectively, in neon matrix (687.8, 685.7, 684.6, 683.0 cm^{-1} in argon matrix) overlaps with either absorptions of IrF_5 or of unknown impurities.

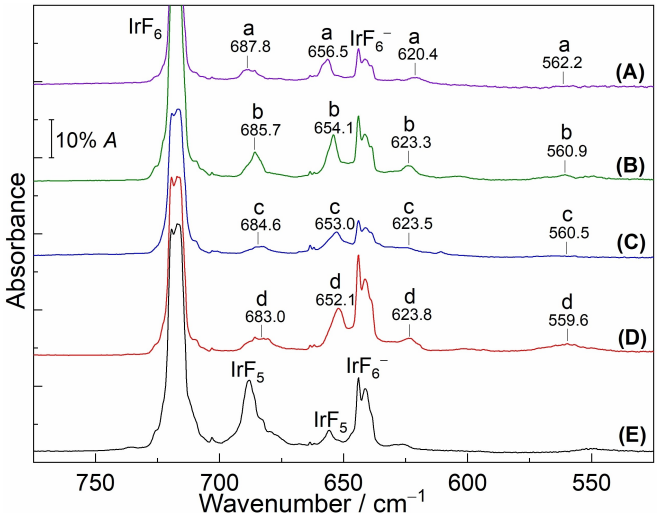

Figure 6. Infrared matrix-isolation spectra of argon matrices at 5 K. (**A**–**D**) Spectra of reaction products of laser-ablated MF (M = Na, K, Rb, Cs) with IrF_6. (**A**) NaF, (**B**) KF, (**C**) RbF and (**D**) CsF. (**E**) Spectrum of the reaction products from laser ablation of Ir with IrF_6. The IR bands of Na[IrF_6], K[IrF_6], Rb[IrF_6], Cs[IrF_6] were labeled with **a**, **b**, **c**, and **d**, respectively.

The assignment of the stretching bands of M[IrF_6] (M = Na, K, Rb, Cs) ion pairs in C_{3v} symmetry was further supported by 2c-X2C DFT calculations including SOC (Tables 2 and S9–S12). Analogous to the case of isolated IrF_6^-, use of a Kramers-restricted pseudo-closed-shell ground state at 2c-X2C level provides best agreement with the observed values. Additionally, in the series of spectra from NaF to CsF, the observed red-shifts of Ir–F vibrational stretching bands in neon matrices at 695.2–686.4 cm^{-1} (687.8–683.0 cm^{-1} in argon), at 661.9–656.7 cm^{-1} (656.5–652.1 cm^{-1} in argon) and at 557.3–556.9 cm^{-1} (562.2–559.6 cm^{-1} in argon), and the blue-shift of the bands at 617.3–620.2 cm^{-1} (620.4–623.8 cm^{-1} in argon) are excellently matched by the trend of the calculated harmonic frequencies, consistent with an increase of the uncoordinated Ir–F bond lengths and a decrease of M-coordinated Ir–F bond lengths in M[IrF_6] from Na to Cs (Table 2 and Figure 1), following the decrease of the Lewis acidity of the alkali cations in the order $Na^+ > K^+ > Rb^+ > Cs^+$.[40]

Since the molecular alkali tetrafluorido aurate M[AuF_4] (M=K, Rb, Cs) ion pairs could be previously generated by the reaction of laser-ablation MF and AuF_3 in solid neon,[32] we have also considered the M[IrF_7] ion pairs for the alkali-metal dependent bands mentioned above. However, M[IrF_7] ion pairs can be ruled out safely, because the alkali-metal dependent bands assigned to M[IrF_6] were also observed in experiments of laser-ablated alkali metal chlorides MCl with IrF_6 (Figure S7). This also prompted us to consider the possible product IrF_7 and its anion IrF_7^- by adding an F atom or a F^- anion to IrF_6, so far

Table 2. Calculated and experimentally observed IR wavenumbers (in cm^{-1}) of M[IrF_6] (M = Na, K, Rb, Cs) ion pairs.[a]

Species	Sym.	Calc. (Int.)[b] 2c-X2C-PBE0 (pseudo-$^1A_1$, C_{3v})	Exp. Ne	Exp. Ar
Na[IrF_6]	a_1	713.4 (76)	695.2	687.8
	e	682.7 (155)×2	661.9	656.5
	a_1	619.9 (148)	617.3	620.4
	e	567.0 (54)×2	557.3	562.2
K[IrF_6]	a_1	707.4 (78)	689.4	685.7
	e	674.5 (169)×2	658.4	654.1
	a_1	622.5 (167)	620.0	623.3
	e	563.0 (40)×2	557.2	560.9
Rb[IrF_6]	a_1	706.4 (81)	687.6	684.6
	e	673.5 (167)×2	657.4	653.0
	a_1	623.2 (175)	620.1	623.5
	e	563.2 (37)×2	557.1	560.5
Cs[IrF_6]	a_1	704.8 (84)	686.4	683.0
	e	672.0 (164)×2	656.7	652.1
	a_1	624.1 (186)	620.2	623.8
	e	563.0 (32)×2	556.9	559.6

[a] The complete set of calculated frequencies is provided in Supporting Information (Tables S9–S12). Intensities are shown in parentheses in km mol^{-1}. [b] Values calculated at 2c-X2C-PBE0-D3(BJ) level with x2c-TZVPall-2c basis set.

only investigated in computational studies.[10] The pentagonal-bipyramidal (D_{5h} symmetry) structure of IrF_7 in a pseudo-triplet ground state has been reported previously in one- and two-component all electron DFT calculations. Its predicted vibrational frequencies would be located at 718 and 662 cm^{-1} with an intensity ratio of 2:3.[37,41] It was also reported that addition of F^- to IrF_6 leads to a $^2B_1/C_{2v}$ structure for the anion IrF_7^- computed at scalar-relativistic B3LYP/aug-cc-pVTZ-PP level,[10] which is consistent with our calculations at 1c-X2C level (Figure S3 and Table S7). Inclusion of SOC in 2c-X2C calculations provides a pentagonal-bipyramidal structure with D_{5h} symmetry for this anion (Figure S4 and Table S8). However, the alkali-metal independent absorptions of either IrF_7 or IrF_7^- were not observed in our experiments.

Since the SOC contribution is essential for predicting the electron affinities for 5d metal hexafluorides,[10] 2c-X2C-DFT calculations including SOC effects were carried out for the electron affinities (EAs) and fluoride ion affinities (FIAs) of IrF_6 and IrF_5 (Table 3). The corresponding 1c-X2C-DFT values without SOC contribution are given in Supporting Information (Table S13). Various bond dissociation energies (BDEs) of IrF_6^-, IrF_7^- anions and $M[IrF_6]$ (M = Na, K, Rb, Cs) ion pairs are shown in Table 4.

Our calculated value of 6.73 eV for the EA of IrF_6 is consistent with the values predicted by theoretical calculations,[10,44,45] but also is in excellent agreement with the experimental value of 6.50±0.38 kcal/mol obtained by using high-temperature Knudsen cell mass spectrometry.[42] Compared to the 1c-X2C–B3LYP value (Table S13), the EA of IrF_6 is increased by 33.8 kJ mol^{-1} at 2c-X2C–B3LYP level (Table 3), slightly more than an earlier reported increase by 25.0 kJ mol^{-1}.[10] However, inclusion of SOC effects gives much smaller effects (2.9 kJ mol^{-1}) for the EA of IrF_5 in the present calculations. The high EAs of 5.81 and 6.73 eV for IrF_5 and IrF_6 sufficiently exceed those of the halogens (3.0–3.6 eV), suggesting that both molecules fall in the category of "superhalogens".[46] Moreover, both EAs also are dramatically larger than those of CCl_4 (2.00±0.20 eV),[47] which serves as electron trapping agent in matrix isolation experiments.[27,48] Hence, the neutral precursor IrF_6 and the photodissociation product IrF_5 should each be able to capture an electron and form IrF_6^- and IrF_5^- anions, respectively, trapped in inert noble-gas matrices. Our 2c-X2C–B3LYP calculated value of 496.0 kJ mol^{-1} for the FIA of IrF_5 is lower than those of 563.2 kJ mol^{-1} calculated by Dixon.[10] Based on the high FIA value, IrF_5 was proposed as an strong Lewis acid. The FIA of IrF_5 is substantially larger (by 244.5 kJ mol^{-1}) than that of IrF_6, but the order of the EA values is reversed.

The Ir–F BDE of IrF_6^- is predicted to be 365.3 kJ mol^{-1}, consistent with the observed stability of these anions. In contrast, the predicted low BDE of 31.5 kJ mol^{-1} for IrF_7^- (slightly lower than a previously computed value of 42.7 kJ mol^{-1})[10] suggests that IrF_7^- is less stable and difficult to prepare in our experiments. The computational results show that the ion-pair BDEs of $M[IrF_6]$ (M = Na, K, Rb, Cs) decrease from $Na[IrF_6]$ (476.3 kJ mol^{-1}) to $Cs[IrF_6]$ (388.6 kJ mol^{-1}). These ion pairs should thus be stable with respect to loss of an alkali-metal ion.

Conclusions

We have reported for the first-time matrix IR spectra of the molecular IrF_5^- and IrF_6^- anions and of the $M[IrF_6]$ (M = Na, K, Rb and Cs) ion pairs stabilized under cryogenic conditions in neon and argon matrices. These species were produced during the laser ablation of different alkali-metal fluorides (NaF, KF, RbF, CsF) with excess IrF_6 in neon or argon at 5 K. However, attempts to prepare IrF_7, the IrF_7^- anion, or its ion pairs $M[IrF_7]$ by this method failed. The alkali-metal independent anions IrF_5^- and IrF_6^- were formed either via electron capture during the laser ablation process, or via the laser ablation of different metals (Ir or Pt) and their reaction with IrF_6. Scalar-relativistic computations (1c-X2C) would predict a D_{4h} structure in a triplet ground state for IrF_6^-, but the calculated frequencies do not match the observed absorptions. The observed single band of IrF_6^- agrees with the predicted frequencies of a Kramer-restricted pseudo-closed-shell ground state with O_h symmetry in the presence of SOC effects at 2c-X2C level. This is in perfect agreement with the energy spectrum obtained from MRCI + Q calculations with SOC. The observed alkali-metal dependent IR absorptions of the Ir–F stretching frequencies for the $M[IrF_6]$ (M = Na, K, Rb, Cs) ion pairs in C_{3v} symmetry stabilized by an alkali metal coordination to three F atoms on one face of the anion are consistent with the structural changes of these complexes when varying the alkali-metal ions from Na to Cs in the computations.

Table 3. Calculated electron affinities (EAs) and fluoride ion affinities (FIAs) at 2c-X2C–B3LYP level.

Species	Calculated[a]		Experiment	Reported values	
	EA [eV]	FIA [kJ mol^{-1}]	EA [eV]	EA [eV]	FIA [kJ mol^{-1}]
IrF_5	5.81	496.0		5.75[c]	563.2[d]
IrF_6	6.73	251.5	6.50 ±0.38[b]	5.99,[d] 5.34,[e] 7.2[f]	292.9[d]

[a] Calculated value in this work at 2c-X2C–B3LYP/x2c-TZVPall-2c level with additional diffuse basis functions for fluorine. [b] Ref.[42]. [c] Ref.[43]. [d] Ref.[10]. [e] Ref.[44]. [f] Ref.[45].

Table 4. Computed bond dissociation energies (BDEs) of IrF_6^-, IrF_7^- and $M[IrF_6]$ ion pairs (298.15 K, kJ mol^{-1}) at 2c-X2C-DFT level.

Process	$\Delta E + \Delta ZPE$	$\Delta_r H$	$\Delta_r G$
$IrF_6^- \rightarrow IrF_5^- + F$[a]	366.4	365.3	365.2
$IrF_7^- \rightarrow IrF_6^- + F$[a]	34.3	31.5	38.2
$Na[IrF_6] \rightarrow IrF_6^- + Na^+$[b]	480.8	476.3	486.3
$K[IrF_6] \rightarrow IrF_6^- + K^+$[b]	425.4	420.1	433.9
$Rb[IrF_6] \rightarrow IrF_6^- + Rb^+$[b]	412.2	406.6	423.6
$Cs[IrF_6] \rightarrow IrF_6^- + Cs^+$[b]	394.6	388.6	408.1

[a] 2c-X2C–B3LYP/x2c-TZVPall-2c level. [b] 2c-X2C-PBE0-D3(BJ)/x2c-TZVPall-2c level.

Experimental and Computational Details

The techniques of matrix-isolation infrared (IR) spectroscopy and the laser-ablation apparatus have been described in more detail in previous works.[5,28,37] The alkali-metal fluoride powder MF (M = Na, K, Rb, Cs) was pressed into a cylindric pellet using a hydraulic lab press. The pellet was subsequently mounted onto a rotatable target holder with a magnetic bearing motor and was transferred into a self-built matrix chamber. The Nd:YAG laser fundamental (Continuum, Minilite II, 1064 nm, 10 Hz repetition Rate, 45–50 mJ pulse^{-1}) was focused onto the alkali metal fluoride or metal (Ir or Pt) targets, which gave an energetic plasma beam and free electrons reacting with IrF_6 spreading toward a gold-plated mirror cooled to 5 K for neon (99.999%, Air Liquide) and argon (99.999%, Sauerstoffwerk Friedrichshafen) using a closed-cycle helium cryostat (Sumitomo Heavy Industries, RDK-205D) inside the matrix chamber. The infrared spectra were recorded on a Bruker Vertex 80v with 0.5 cm^{-1} resolution in the region 4000–450 cm^{-1} by using a liquid-nitrogen-cooled mercury cadmium telluride (MCT) detector. Matrix samples were annealed to 9 K and irradiated by selected light-emitting diode (LED) sources ($\lambda = 656 \pm 10$ nm).

Preparation of iridium hexafluoride followed procedures described in the literature.[49] It was prepared by heating iridium metal powder in a stainless-steel autoclave with an excess of fluorine at 300 °C for about 8 h. The product IrF_6 was stored in a fluoroplastic (PFA) tube, trapped by liquid nitrogen. It was further purified by long pumping, and its initial purity was monitored by IR spectroscopy. After purification, the gas sample was mixed by passing a stream of neon or argon gas through a cold PFA tube (−96 °C) containing the IrF_6 sample and deposited on the matrix support for measurements.

As relativistic effects are known to be crucial for the description of Ir complexes, quasi-relativistic all-electron DFT calculations using the "exact-two-component" (X2C) Hamiltonian were performed at one-component and Kramers-restricted two-component (1c-X2C and 2c-X2C)[33,50] levels, using either the B3LYP[51] or PBE0[52] functionals, x2c-TZVPall-2c all-electron basis sets,[53] and a very fine quadrature grid (TURBOMOLE gridsize m5). For the calculation of fluoride ion affinities, the x2c-TZVPall-2c basis set of fluorine was supplemented by additional diffuse basis functions taken from the def2-TZVPD basis set.[54] These calculations were done with Turbomole 7.4.1.[55] For the M[IrF_6] (M = Na, K, Rb, Cs) ion pairs, additional dispersion corrections were included using Grimme's DFT–D3[56] scheme with Becke–Johnson (BJ) damping[57] and the parameters for either B3LYP or PBE0. Two-electron SOC terms were approximated using the scaled-nuclear-spin-orbit (SNSO)[58] approach in its original parameterization by Boettger.[59] A finite-nucleus model was used in all calculations.[60]

Additional calculations at the MRCI level[34,35] were performed with the MOLPRO program, Version 2022.2[61] All calculations employed the 1c-X2C Hamiltonian, ANO-RCC basis sets,[62] and D_{2h} symmetry. MRCI + Q calculations were performed based on state-averaged CASSCF calculations with an active space of 8 electrons in 7 orbitals, containing the five 5d orbitals of Ir and the two symmetrically adapted ligand orbitals of (formal) e_g symmetry. State-averaging was performed over all components of the lowest crystal field states ($^1T_{2g}$, ^1E_g, $^1A_{1g}$, $^3T_{1g}$ and ^5E_g). Spin-orbit coupling eigenstates were obtained by diagonalization of the sum of the electronic and the Breit-Pauli SOC Hamiltonian in the basis of the MRCI wave functions obtained for all states mentioned above.[36] The energy eigenvalues of the electronic Hamiltonian were adapted to include the Davidson size-consistency correction (+Q)[63] using a relaxed reference.

Supporting Information

The authors have cited additional references within the Supporting Information.[2,5]

Acknowledgements

We gratefully acknowledge the Zentraleinrichtung für Datenverarbeitung (ZEDAT) of the Freie Universität Berlin for the allocation of computing resources.[64] Computations at Technische Universität Berlin used local resources at the Faculty II computing center. We thank the ERC Project HighPotOx as well as the CRC 1349 (SFB 1349) Fluorine-Specific Interactions-Project-ID 387284271 for continuous support. Y. L. thanks the China Scholarship Council (PhD Program) for financial support. Open Access funding enabled and organized by Projekt DEAL.

Conflict of Interests

The authors declare no conflict of interest.

Data Availability Statement

The data that support the findings of this study are available from the corresponding author upon reasonable request.

Keywords: IR spectroscopy · matrix isolation · d^4 transition-metal compounds · spin-orbit coupling · quantum chemistry

[1] A. V. Wilson, T. Nguyen, F. Brosi, X. Wang, L. Andrews, S. Riedel, A. J. Bridgeman, N. A. Young, *Inorg. Chem.* **2016**, *55*, 1108.
[2] L. Alvarez-Thon, J. David, R. Arratia-Pérez, K. Seppelt, *Phys. Rev. A* **2008**, *77*, 34502.
[3] a) S. P. Gabuda, S. G. Kozlova, *Phys. Rev. A* **2009**, *79*, 056501; b) G. Aullon, S. Alvarez, *Inorg. Chem.* **2007**, *46*, 2700; c) F. Wöhler, *Ann. Chim. Phys.* **1828**, *37*, 101.
[4] J. David, P. Fuentealba, A. Restrepo, *Chem. Phys. Lett.* **2008**, *457*, 42.
[5] G. Senges, L. Li, A. Wodyński, H. Beckers, R. Müller, M. Kaupp, S. Riedel, *Chem. Eur. J.* **2021**, *27*, 13642.
[6] K. Seppelt, *Chem. Rev.* **2015**, *115*, 1296.
[7] R. Craciun, R. T. Long, D. A. Dixon, K. O. Christe, *J. Phys. Chem. A* **2010**, *114*, 7571.
[8] S. P. Gabuda, V. N. Ikorskii, S. G. Kozlova, P. S. Nikitin, *JETP Lett.* **2001**, *73*, 35.
[9] A. A. Timakov, V. N. Prusakov, Y. V. Drobyshevskii, *Zh. Neorg. Khim.* **1982**, *27*, 3007.
[10] R. Craciun, D. Picone, R. T. Long, S. Li, D. A. Dixon, K. A. Peterson, K. O. Christe, *Inorg. Chem.* **2010**, *49*, 1056.
[11] W. Moffitt, G. L. Goodman, M. Fred, B. Weinstock, *Mol. Phys.* **1959**, *2*, 109.
[12] J. H. Holloway, G. Stanger, E. G. Hope, W. Levason, J. S. Ogden, *J. Chem. Soc. Dalton Trans.* **1988**, 1341.
[13] R. Fernandes De Farias, *Inorg. Chem.* **2016**, *55*, 12126.
[14] J. David, D. Guerra, A. Restrepo, *Inorg. Chem.* **2011**, *50*, 1480.
[15] G. C. Allen, G. A. M. El-Sharkawy, K. D. Warren, *Inorg. Chem.* **1972**, *11*, 51.
[16] S. Seidel, K. Seppelt, *Angew. Chem. Int. Ed.* **2000**, *39*, 3923.
[17] A. Earnshaw, B. N. Figgis, J. Lewis, R. D. Peacock, *J. Chem. Soc.* **1961**, 3132.
[18] a) S. I. Ivlev, K. Gaul, M. Chen, A. J. Karttunen, R. Berger, F. Kraus, *Chem. Eur. J.* **2019**, *25*, 5793; b) B. Scheibe, A. J. Karttunen, F. Kraus, *Eur. J. Inorg. Chem.* **2021**, *2021*, 405; c) M. A. Hepworth, K. H. Jack, G. J. Westland, *J.*

Inorg. Nucl. Chem. **1956**, *2*, 79; d) R. D. W. Kemmitt, D. R. Russell, D. W. A. Sharp, *J. Chem. Soc.* **1963**, 4408; e) D. H. Brown, D. R. Russell, D. W. A. Sharp, *J. Chem. Soc. A* **1966**, 18.
[19] O. Graudejus, A. P. Wilkinson, L. C. Chacon, N. Bartlett, *Inorg. Chem.* **2000**, *39*, 2794.
[20] H. Fitz, B. G. Muller, O. Graudejus, N. Bartlett, *Z. Anorg. Allg. Chem.* **2002**, *628*, 133.
[21] Z. Mazej, E. Goreshnik, K. O. Christe, *J. Fluorine Chem.* **2023**, *268*, 110128.
[22] Z. Mazej, R. Hagiwara, *J. Fluorine Chem.* **2007**, *128*, 423.
[23] a) K. S. Pedersen, J. Bendix, A. Tressaud, E. Durand, H. Weihe, Z. Salman, T. J. Morsing, D. N. Woodruff, Y. Lan, W. Wernsdorfer, C. Mathonière, S. Piligkos, S. I. Klokishner, S. Ostrovsky, K. Ollefs, F. Wilhelm, A. Rogalev, R. Clérac, *Nat. Commun.* **2016**, *7*, 12195; b) A. I. Gubanov, A. I. Smolentsev, E. Filatov, N. V. Kuratieva, A. M. Danilenko, S. V. Korenev, *ACS Omega* **2021**, *6*, 27697; c) M. Rossi, M. Retegan, C. Giacobbe, R. Fumagalli, A. Efimenko, T. Kulka, K. Wohlfeld, A. I. Gubanov, M. Moretti Sala, *Phys. Rev. B* **2017**, *95*, 235161.
[24] a) N. Bartlett, S. P. Beaton, N. K. Jha, *Chem. Commun.* **1966**, 168; b) N. Bartlett, *Angew. Chem. Int. Ed.* **1968**, *7*, 433.
[25] T. Vent-Schmidt, F. Brosi, J. Metzger, T. Schlöder, X. Wang, L. Andrews, C. Müller, H. Beckers, S. Riedel, *Angew. Chem. Int. Ed.* **2015**, *54*, 8279.
[26] S. Riedel, T. Köchner, X. Wang, L. Andrews, *Inorg. Chem.* **2010**, *49*, 7156.
[27] L. Zhang, J. Dong, M. Zhou, Q. Qin, *J. Chem. Phys.* **2000**, *113*, 10169.
[28] F. A. Redeker, H. Beckers, S. Riedel, *Chem. Commun.* **2017**, *53*, 12958.
[29] M. Zhou, L. Zhang, Q. Qin, *J. Am. Chem. Soc.* **2000**, *122*, 4483.
[30] F. Brosi, T. Vent-Schmidt, S. Kieninger, T. Schlöder, H. Beckers, S. Riedel, *Chem. Eur. J.* **2015**, *21*, 16455.
[31] F. A. Redeker, H. Beckers, S. Riedel, *RSC Adv.* **2015**, *5*, 106568.
[32] F. A. Redeker, M. A. Ellwanger, H. Beckers, S. Riedel, *Chem. Eur. J.* **2019**, *25*, 15059.
[33] A. Baldes, F. Weigend, *Mol. Phys.* **2013**, *111*, 2617.
[34] H.-J. Werner, P. J. Knowles, *J. Chem. Phys.* **1988**, *89*, 5803.
[35] P. J. Knowles, H.-J. Werner, *Chem. Phys. Lett.* **1988**, *145*, 514.
[36] A. Berning, M. Schweizer, H.-J. Werner, P. J. Knowles, P. Palmieri, *Mol. Phys.* **2000**, *98*, 1823.
[37] Y. Lu, Y. A. Tsegaw, A. Wodyński, L. Li, H. Beckers, M. Kaupp, S. Riedel, *Chem. Eur. J.* **2022**, *28*, e202104005.
[38] G. Herzberg, *Molecular Spectra and Molecular Structure: III. Electronic Spectra and Electronic Structure of Polyatomic Molecules*, Van Nostrand Reinhold, New York, **1966**, pp. 296–350.
[39] X. Wang, L. Andrews, F. Brosi, S. Riedel, *Chem. Eur. J.* **2013**, *19*, 1397.
[40] R. C. Deka, R. Kinkar Roy, K. Hirao, *Chem. Phys. Lett.* **2004**, *389*, 186.
[41] S. Riedel, M. Kaupp, *Angew. Chem. Int. Ed.* **2006**, *45*, 3708.
[42] M. V. Korobov, S. V. Kuznetsov, L. N. Sidorov, V. A. Shipachev, V. N. Mit'kin, *Int. J. Mass Spectrom. Ion Processes* **1989**, *87*, 13.
[43] S. A. Macgregor, K. H. Moock, *Inorg. Chem.* **1998**, *37*, 3284.
[44] G. L. Gutsev, A. I. Boldyrev, *Chem. Phys. Lett.* **1983**, *101*, 441.
[45] S. A. Siddiqui, T. Rasheed, *Int. J. Quantum Chem.* **2013**, *113*, 959.
[46] G. L. Gutsev, A. I. Boldyrev, *Chem. Phys.* **1981**, *56*, 277.
[47] a) H. Dispert, K. Lacmann, *Int. J. Mass Spectrom. Ion Phys.* **1978**, *28*, 49; b) K. Lacmann, M. J. P. Maneira, A. M. C. Moutinho, U. Weigmann, *J. Chem. Phys.* **1983**, *78*, 1767.
[48] M. Zhou, L. Andrews, *J. Am. Chem. Soc.* **1998**, *120*, 11499.
[49] A. D. Richardson, K. Hedberg, G. M. Lucier, *Inorg. Chem.* **2000**, *39*, 2787.
[50] a) M. K. Armbruster, F. Weigend, C. van Wüllen, W. Klopper, *Phys. Chem. Chem. Phys.* **2008**, *10*, 1748; b) D. Peng, N. Middendorf, F. Weigend, M. Reiher, *J. Phys. Chem.* **2013**, *138*, 184105.
[51] a) P. J. Stephens, F. J. Devlin, C. F. Chabalowski, M. J. Frisch, *J. Phys. Chem.* **1994**, *98*, 11623; b) A. D. Becke, *J. Chem. Phys.* **1993**, *98*, 5648; c) C. Lee, W. Yang, R. G. Parr, *Phys. Rev. B* **1988**, *37*, 785; d) S. H. Vosko, L. Wilk, M. Nusair, *Can. J. Phys.* **1980**, *58*, 1200.
[52] a) C. Adamo, V. Barone, *J. Chem. Phys.* **1999**, *110*, 6158; b) J. P. Perdew, M. Ernzerhof, K. Burke, *J. Chem. Phys.* **1996**, *105*, 9982.
[53] P. Pollak, F. Weigend, *J. Chem. Theory Comput.* **2017**, *13*, 3696.
[54] D. Rappoport, F. Furche, *J. Chem. Phys.* **2010**, *133*, 134105.
[55] a) *Turbomole V7.4.1 2019. a development of University of Karlsruhe and Forschungszentrum Karlsruhe GmbH*, 1989–2007, *TURBOMOLE GmbH, since 2007. Available from:* http://www.turbomole.com; b) S. G. Balasubramani, G. P. Chen, S. Coriani, M. Diedenhofen, M. S. Frank, Y. J. Franzke, F. Furche, R. Grotjahn, M. E. Harding, C. Hättig, A. Hellweg, B. Helmich-Paris, C. Holzer, U. Huniar, M. Kaupp, A. Marefat Khah, S. Karbalaei Khani, T. Müller, F. Mack, B. D. Nguyen, S. M. Parker, E. Perlt, D. Rappoport, K. Reiter, S. Roy, M. Rückert, G. Schmitz, M. Sierka, E. Tapavicza, D. P. Tew, C. van Wüllen, V. K. Voora, F. Weigend, A. Wodyński, J. M. Yu, *J. Phys. Chem.* **2020**, *152*, 184107.
[56] S. Grimme, J. Antony, S. Ehrlich, H. Krieg, *J. Chem. Phys.* **2010**, *132*, 154104.
[57] S. Grimme, S. Ehrlich, L. Goerigk, *J. Comput. Chem.* **2011**, *32*, 1456.
[58] Y. J. Franzke, N. Middendorf, F. Weigend, *J. Chem. Phys.* **2018**, *148*, 104110.
[59] J. C. Boettger, *Phy. Rev. B* **2000**, *62*, 7809.
[60] L. Visscher, K. G. Dyall, *At. Data Nucl. Data Tables* **1997**, *67*, 207.
[61] a) H.-J. Werner, P. J. Knowles, F. R. Manby, J. A. Black, K. Doll, A. Heßelmann, D. Kats, A. Köhn, T. Korona, D. A. Kreplin, Q. Ma, T. F. Miller III, A. Mitrushchenkov, K. A. Peterson, I. Polyak, G. Rauhut, M. Sibaev, *J. Chem. Phys.* **2020**, *152*, 144107; b) H.-J. Werner, P. J. Knowles, G. Knizia, F. R. Manby, M. Schütz, P. Celani, W. Györffy, D. Kats, T. Korona, R. Lindh, A. Mitrushenkov, G. Rauhut, K. R. Shamasundar, T. B. Adler, R. D. Amos, S. J. Bennie, A. Bernhardsson, A. Berning, D. L. Cooper, M. J. O. Deegan, A. J. Dobbyn, F. Eckert, E. Goll, C. Hampel, A. Hesselmann, G. Hetzer, T. Hrenar, G. Jansen, C. Köppl, S. J. R. Lee, Y. Liu, A. W. Lloyd, Q. Ma, R. A. Mata, A. J. May, S. J. McNicholas, W. Meyer, T. F. Miller III, M. E. Mura, A. Nicklass, D. P. O'Neill, P. Palmieri, D. Peng, T. Petrenko, K. Pflüger, R. Pitzer, M. Reiher, T. Shiozaki, H. Stoll, A. J. Stone, R. Tarroni, T. Thorsteinsson, M. Wang, M. Welborn, *Molpro, version 2022.2. a package of ab initio programs* http://www.molpro.net.
[62] a) B. O. Roos, R. Lindh, P.-A. Malmqvist, V. Veryazov, P.-O. Widmark, *J. Phys. Chem. A* **2005**, *109*, 6575; b) B. O. Roos, R. Lindh, P.-Å. Malmqvist, V. Veryazov, P.-O. Widmark, *J. Phys. Chem. A* **2004**, *108*, 2851.
[63] S. R. Langhoff, E. R. Davidson, *Int. J. Quantum Chem.* **1974**, *8*, 61.
[64] L. Bennett, B. Melchers, B. Proppe, *Curta: A General-purpose High-Performance Computer at ZEDAT, Freie Universität Berlin*, Freie Universität Berlin, **2020**.

Manuscript received: March 12, 2024
Accepted manuscript online: April 15, 2024
Version of record online: May 17, 2024